Research Article

Weiwei Li, Can Ge*, Fangyue Wang, He Sun, and Haiou Gu

The spatial distribution characteristics of Nb–Ta of mafic rocks in subduction zones

https://doi.org/10.1515/geo-2020-0242
received July 28, 2020; accepted March 09, 2021

Abstract: High field-strength elements have been regarded as one of the most important discriminations in subduction zone magma. However, the spatial distribution of Nb and Ta in subduction zone-related rocks has been rarely studied; it is still unclear whether there is a quantitative relationship between the Nb–Ta concentrations and their subduction distance. In this paper, the Nb–Ta concentrations of mafic rocks in arc tectonic systems were calculated from a statistical perspective based on the combined geophysical model and geochemical database. The results showed a typical spatial distribution pattern. The threshold value of Nb (12.20 ppm) and Ta (0.796 ppm) in arc settings was estimated by a cumulative distribution function, which can be used to determine whether the rock is generated in arc tectonic environment. A probability density function of Nb–Ta contents and related subduction distance has been obtained using kernel function estimation. The Nb–Ta concentrations are exponentially correlated with the subduction distance (<700 km), while the Nb/Ta ratios keep in the range of 12–19. We proposed that the subduction depth, along with the degree of partial melting, and possible crustal contamination might be responsible for the Nb–Ta variation correlation with subduction distances.

Keywords: mafic rocks, Nb–Ta, spatial distribution, geochemical characteristics, subduction zones

1 Introduction

In the solar system, Earth is the only planet that does have plate tectonics, which is the main process to trigger magma evolution, differentiation, and elemental cycling. As the main areas for plate demise and magmatism arise, magmatism in subduction zones is closely related to the exchange of matter and energy between the crust and the mantle [1–8]. Meanwhile, many studies have focused on the growth of continental crust (CC) and the role of arc magmatism, modern subduction zone architecture, systematics, magma genesis, and geochemical variations within the products of continental and island arc magmas [8–20]. Geophysical studies (e.g., seismic wave, geomagnetism, and geo-electricity) can offer the angle at which the plate is being subducted and distance of the subduction zone from continental margins, and geochemical studies reveal the composition of subducting material and involved mechanism in subduction zones, both leading to a better understanding of the subduction zone processes. The inhomogeneity of elements in different layers of our Earth is influenced by events such as oceanic ridge expansion, plate subduction, and magma evolution under different physical–chemical conditions [21–24]. Therefore, the elemental distributions in different Earth reservoirs can be an effective probe to understand our Earth. Subduction zone-related interplate and intraplate mafic rocks are products of mantle sourced magmas that contain the geochemical signature of crustal components. Several groups of trace elements, such as large ion lithophile elements, light rare Earth elements, heavy rare Earth elements, and high field-strength elements (HFSE), have been used to trace and decipher the subduction processes

* **Corresponding author: Can Ge,** School of Resources and Environmental Engineering, Hefei University of Technology, No. 193 Tunxi Road, Baohe District, Hefei 230009, Anhui, China; Anhui Province Engineering Research Center for Mineral Resources and Mine Environments, Hefei University of Technology, No. 193 Tunxi Road, Baohe District, Hefei 230009, Anhui, China; Ore Deposit and Exploration Centre (ODEC), Hefei University of Technology, No. 193 Tunxi Road, Baohe District, Hefei 230009, Anhui, China, e-mail: gecan@hfut.edu.cn, tel: +86-183-2666-8551
Weiwei Li, Fangyue Wang, He Sun, Haiou Gu: School of Resources and Environmental Engineering, Hefei University of Technology, No. 193 Tunxi Road, Baohe District, Hefei 230009, Anhui, China; Anhui Province Engineering Research Center for Mineral Resources and Mine Environments, Hefei University of Technology, No. 193 Tunxi Road, Baohe District, Hefei 230009, Anhui, China; Ore Deposit and Exploration Centre (ODEC), Hefei University of Technology, No. 193 Tunxi Road, Baohe District, Hefei 230009, Anhui, China

on account of their unique geochemical properties. Of these trace elements, HFSEs (e.g., Th, U, Zr, Ti, Nb, Ta, and Hf) are relatively stable and are immobile during metamorphism, alteration, and weathering, and therefore can serve as valid tracers for the magmatic process. These elements were used to trace magma sources and geological process [16,25–39]. As typical HFSEs, element niobium (Nb) and element tantalum (Ta) have long been regarded as geochemical "identical twins," as they have similar ionic radius and electronic structures. They are linked with the elemental balance of the Earth and the growth mechanism of the CC [38]. Previous studies focused on different Nb–Ta minerals occurrence state, the Nb–Ta concentrations in minerals and rocks, and the Nb/Ta ratios [25,27,36,40–43]. However, the spatial distribution of Nb–Ta concentrations and their ratios in subduction zones has long been overlooked in previous studies. In the past decade, the establishment and refinement of the global geochemical databases have provided effective means for big data analysis and statistics in Earth sciences [44]. By analyzing the geochemical characteristic of global rocks, patterns can be found in the distribution of elements in different tectonic settings [45–47].

In this study, based on the global geochemical data set of mafic rocks (0–5 Ma) in typical arc-continent systems, the spatial distribution characteristics of Nb–Ta were investigated, and cumulative distribution function (CDF) was used to obtain the threshold value of Nb and Ta in arc tectonic settings (12.20 ppm and 0.796 ppm). It can be fitted that the Nb and Ta concentrations are exponentially correlated with the subduction distance, with the values of Nb/Ta ratios, however, stay stable. The data characteristics implied that the subduction distance, which may be directly related to the subduction depth, may provide a first-order explanation for the observed distribution patterns for the Nb–Ta concentrations in subduction zones.

2 Data and methods

The geochemical data used in the present study came from EarthChem (Geochemical Databases for the Earth), a well-known international scientific database system in petrology [48,49]. Because the database is not expected to arbitrarily generate from a bias for rocks of a particular age, the geochemical data of igneous rocks from the EarthChem database are representative of global magmatism throughout Earth's history [16]. Therefore, such a database is probably the best means currently for assessing the spatial distribution of geochemical elements in worldwide rocks.

2.1 Data compilation and filtering

The continuous plate tectonic activity on the Earth would constantly change the location of igneous rocks; therefore, ancient rocks, which had been subjected to possible multiple tectonic transformations, are unreliable candidates to represent their geographical locations in subduction zones. The short history of the young rocks (≤5 Ma) makes their occurrence locations reliable to stand for the geographical locations of the geological settings. Therefore, those mafic rocks (45–53 wt% SiO_2) younger than 5 Ma in subduction zones were selected to constrain the Nb–Ta properties during plate subduction.

Rocks in the continental collision zone were discarded first, as these rocks were related to continental subduction processes, where the elements may behave differently from those in the oceanic subduction zones. Rocks from East African Great Rift Valley were not included here for the same reason. The Ocean Island Basalts (OIB), which are far away from subduction zones, are also removed from the data sets. Because these rocks are believed to be derived from mantle plumes [50–52], they are not suitable for the present study. The mafic rocks in western North America were also excluded because they were related to mid-oceanic ridge subduction [53–56]. Such geological process may induce complicated geochemical geodynamical processes of mafic rocks.

2.2 Method

2.2.1 Subduction zone geometry model

Subduction zone model data come from the Slab 2 proposed by Hayes et al. [57]. Slab 2 describes the detailed geometry of more than 24 million square kilometers of subducted slabs; the data for Slab 2 include data distribution (X, Y) and slab depth models (Z) on a regional level. It provides greater global coverage at a finer resolution than previous global subduction zone geometry models [57,58]. We modeled the slab depth at individual nodes over a grid for each subduction zone and then interpolated those depths onto a 3D grid, or surface (Figure 1). According to the depth of subduction zone models, we can get the direction that slab subducted and extract

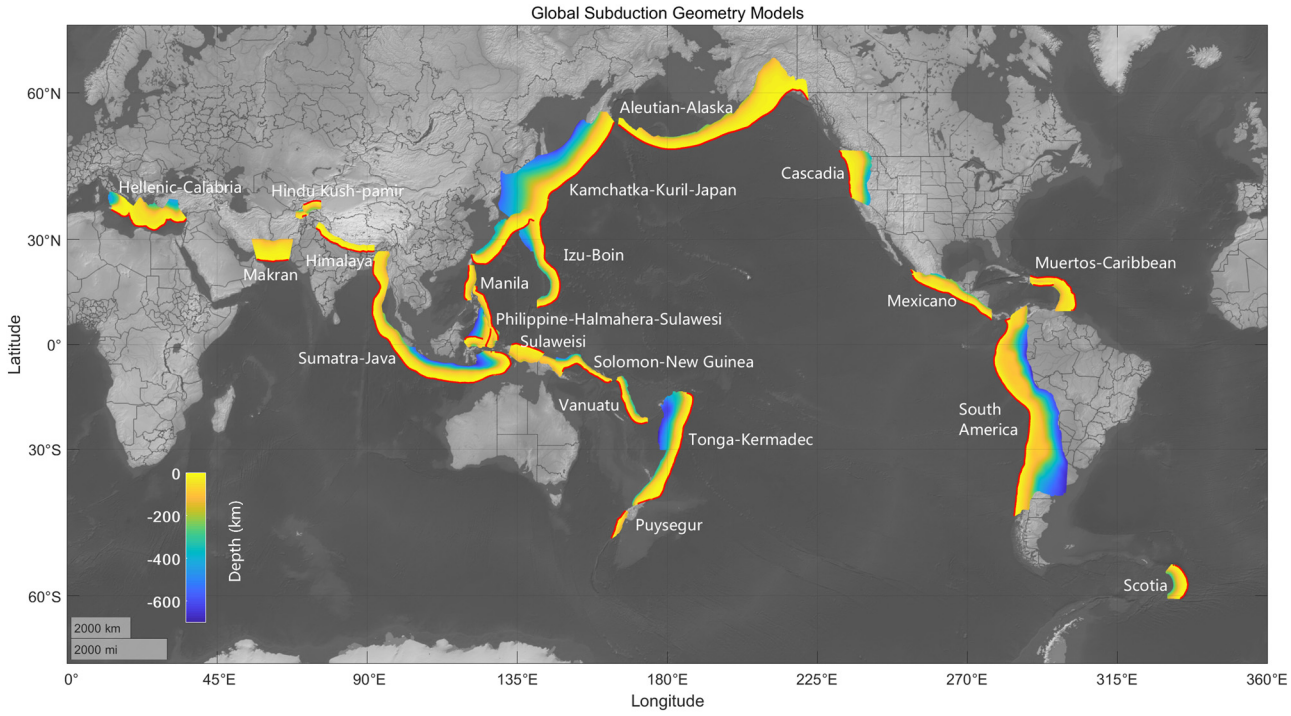

Figure 1: Global subduction geometry models. Data obtained from https://www.sciencebase.gov/catalog/item/5aa1b00ee4b0b1c392e86467.

the data from the outermost beginning of the subduction zone as the boundary line of subduction zone. The shortest distance from mafic rocks to the subduction zone (trench), called "subduction distance" in this paper, is calculated based on the inferior arc length of the great circle from the sample location (longitude and latitude) to the boundary line of subduction zone.

2.2.2 Statistical methods

As geochemical element concentrations are influenced by many factors [59], individual elemental concentrations appear to be random, but there is a clear statistical pattern in the case of a large number of samples. In our study, we used the kernel density estimation method that can be used in probability theory to estimate an unknown density function. The probability density function (PDF) of the Nb–Ta concentrations corresponding to subduction distances from 0 to 2,200 km was calculated using kernel density estimation method; the width of the sample window is set at 200 km subduction distance, while the step width is set at 100 km subduction distance. Mean value and corresponding standard error for every 60 km subduction distance were obtained by calculating the average value and standard deviation of those data sets. The step width is set at 30 km subduction distance.

3 Results

3.1 Characteristics of spatial distribution

As shown in Figure 2, in East Asia and South America, mafic rocks in arc tectonic systems hold relatively low Nb concentrations, while the Nb concentrations of the intracontinental mafic are higher (Figure 2a and b). It is also noteworthy that intracontinental mafic rocks in East Asia are significantly more Nb-enriched than those from South America. Similarly, rocks in typical arc tectonic settings (e.g., Sumatra Island and Vanuatu) have the low Nb concentrations (Figure 2c and d). A similar trend can also be observed in Ta (Figure 2e–h). In arc mafic rocks, the concentrations of Ta are lower than in intracontinental mafic rocks. These observations suggest a systematical difference of Nb–Ta concentrations between arc mafic rocks and intracontinental mafic rocks.

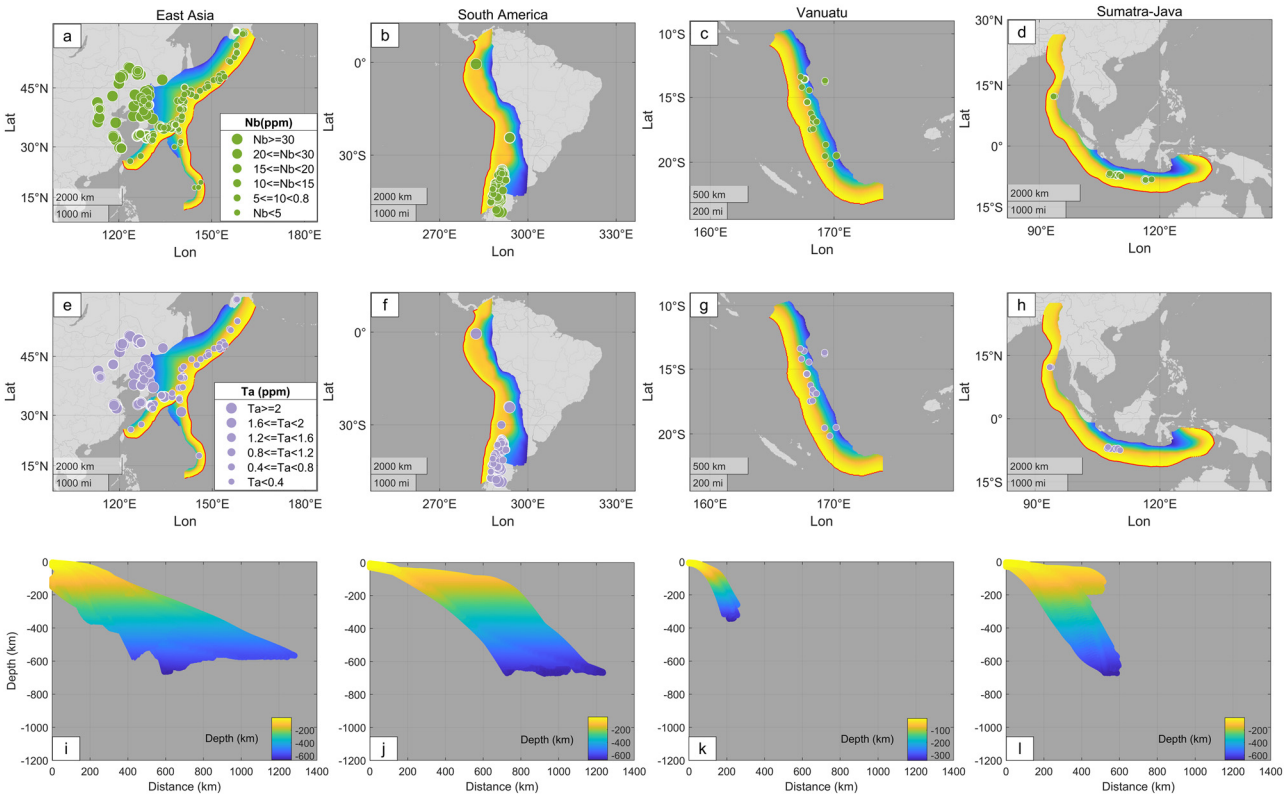

Figure 2: The characteristics of Nb–Ta concentrations of mafic rocks near subduction zone. (a–d) Locations and concentrations of Nb (ppm) of mafic rock samples (0–5 Ma ages, 45–53 wt% SiO_2) in East Asia, South America, Vanuatu, and Sumatra-Java. (e–f) Locations and concentrations of Ta (ppm) of mafic rock samples (0–5 Ma ages, 45–53 wt% SiO_2) in East Asia, South America, Vanuatu, and Sumatra-Java. (i–l) Depth-distance compositional models in East Asia, South America, Vanuatu, and Sumatra-Java. The color bar means the depth of subduction (km), color with yellow means relatively low depth of subduction, and color with blue means the relatively high depth of subduction.

3.2 Threshold value of Nb–Ta in arc tectonic systems

In Figure 3, the element contents (Nb–Ta) of the arc data do not obey a normal distribution. These data points should fall near the Normal CDF 2 (red line) in the figure, but the actual data show that the distribution deviates significantly from the normal distribution. As a result, large biases and misinterpretations will be introduced using traditional means and standard deviations. Therefore, we used the empirical CDF to calculate the cumulative probability of Nb–Ta concentrations of arc and intracontinental mafic rocks. As shown in Figure 3a, 90% of the arc samples have Nb concentrations below 12.20 ppm. In contrast, more than 90% of the intracontinental samples have Nb concentrations above 12.20 ppm. Accordingly, the 12.20 ppm for Nb concentrations was suggested as an empirical reference threshold to distinguish the arc and intracontinental settings. Mafic rocks (<5 Ma) with Nb concentrations above this threshold are less likely to be produced in arc settings, and based on the 95% lower and upper confidence bounds of the empirical CDF, we obtain the threshold upper and lower bounds of 9.20 ppm and 17.68 ppm for Nb concentrations, respectively. In Figure 3b, the classified threshold of Ta in arc systems is 0.796 ppm, and 90% of the arc samples have Ta concentrations below 0.796 ppm, with upper and lower bounds for Ta concentrations of 0.499 ppm and 1.096 ppm, respectively. In general, future big data studies may use the threshold value of Nb–Ta in arc tectonic systems as a reference standard for classifying the rocks from arc or intracontinental tectonic systems preliminarily.

3.3 The relationship of Nb–Ta concentrations and subduction distance

3.3.1 Probability density function

To investigate the relationship between geochemical indicators (Nb–Ta) of mafic rocks and subduction

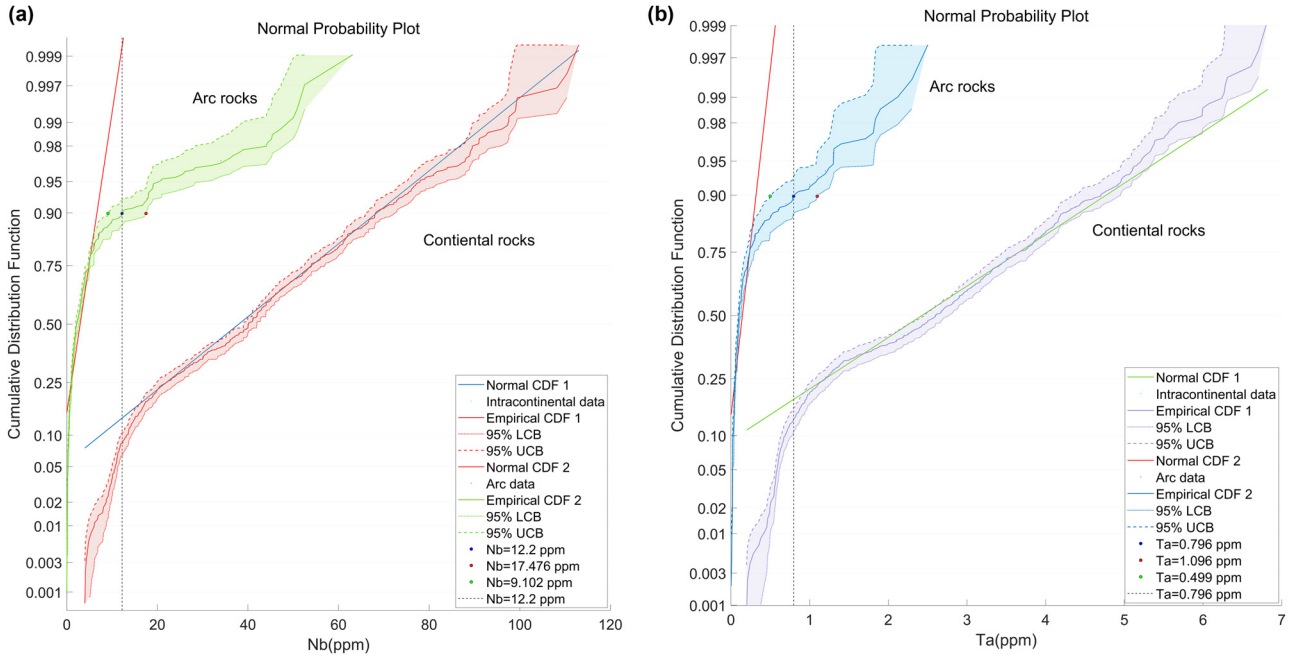

Figure 3: The cumulative distribution function of Nb (a) and Ta concentrations (b) for arc-continent tectonic systems. The green (arc), red (continent), blue (arc), and purple (continent) bands denote 95% lower and upper confidence bounds (CB) of samples. (a) The blue line (normal CDF1) and red line (normal CDF2) denote the normal distribution of Nb concentrations in arc and continent systems, respectively. (b) The green line (normal CDF1) and red line (normal CDF2) denote the normal distribution of Ta concentrations samples in arc and continent systems, respectively. The fold line in bands denotes the cumulative probability of samples based on empirical CDF. Points with green, blue, and red color means the lower limit values, threshold values, and upper limit values of Nb–Ta concentrations in arc tectonic environments, respectively (90% probability).

distance, we calculated the concentrations distribution and mean-standard error distribution, probability density distribution of Nb–Ta at different subduction distance intervals (As shown in Figure 4a and b). It can be used to visualize the distribution of data which is helpful to grasp and summarize the distribution rules of geochemical element contents of mafic rocks at different subduction distance. In different subduction distance intervals, Nb and Ta concentrations of mafic rocks have different trends. All the Nb and Ta concentrations varied over a small range before ~350 km. Such a region is dominated by arc mafic rocks with the Nb–Ta concentrations. Both Nb and Ta concentrations show a rapid increase in trends with subduction distance from 350 to 700 km. A decrease in Nb and Ta concentrations can be seen in subduction distances between 700 and 1,200 km. After 1,200 km, Nb and Ta concentrations keep at high values with relatively small fluctuations. According to the depth-distance models (Figure 2i–l), slab depth (>700 km) and slab extend distance (>1,300 km) of subduction zone geometry models have few reliable records [57,60–62]. When the distance from mafic rocks to the boundary subduction zone is higher than 1,300 km, magmatism may play a lesser role in controlling the concentrations of elements (Nb–Ta) of those mafic rocks.

3.3.2 The regression equation of Nb–Ta and subduction distance

The current slab models are not available after a certain distance (>1,300 km) and depth (>700 km). There is a difficulty in fitting the relationship with the whole data. Therefore, the data from 0 to 700 km of subduction distance were extracted to establish a function of subduction distance. The results show that all the Nb and Ta concentrations of mafic rocks increase as subduction distance increases from 0 to 700 km (Figure 5a and b). The corresponding fit equations were obtained by regression analysis (see equations (1) and (2)). The R^2 values of the Nb and Ta regression equation were 0.679 and 0.773, respectively, which can be considered statistically significant correlations. It suggests that the content of Nb and Ta in mafic rocks increases as the subduction distance increases during the subduction scenario.

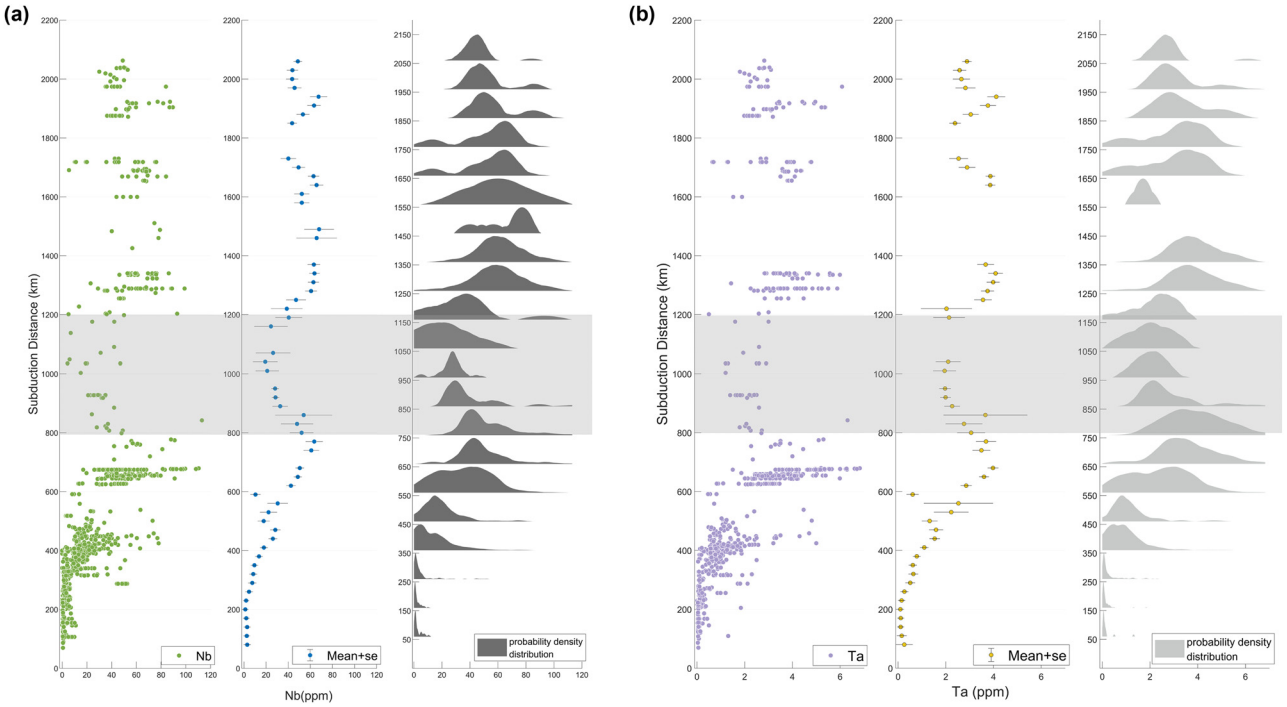

Figure 4: Concentrations distribution, mean values distribution, and probability density distribution of Nb (a) and Ta (b) trends in mafic rocks. The mean values are applied with the window width equal to 60 km, while the moving step width is 30 km. Error bars denote one standard error of the mean (SEM). The light gray and dark gray bands are the PDF estimated using kernel density estimation method. The window width is 100 km, and the moving step width is 50 km.

$$\mathcal{Y} = 2.326 \times e^{0.004617 \times \mathcal{X}} \quad (\mathcal{R}^2 = 0.6797), \tag{1}$$

$$\mathcal{Y} = 0.101 \times e^{0.005478 \times \mathcal{X}} \quad (\mathcal{R}^2 = 0.7733). \tag{2}$$

3.3.3 The Nb/Ta ratios

As an important element pair, the ratio between Nb and Tb can be used as a geochemical indicator to trace source materials for magmatic systems [38]. The change of Nb/Ta ratios is an important research field for the formation and evolution of CC [25,26,30,38,63]. Terrestrial major geochemical reservoirs may have distinct Nb/Ta ratios, such as CC has relatively low Na/Ta ratios at ~12 [12,38] while depleted mantle (DM) has relatively high Nb/Ta ratios of ~15 [27,64,65], and the Nb/Ta ratios from island arc basalt in Kamchatka is 11.3 to 17.8 [66]. In this paper, the Nb/Ta ratios are 12 to 19 in mafic rocks (<2,200 km),

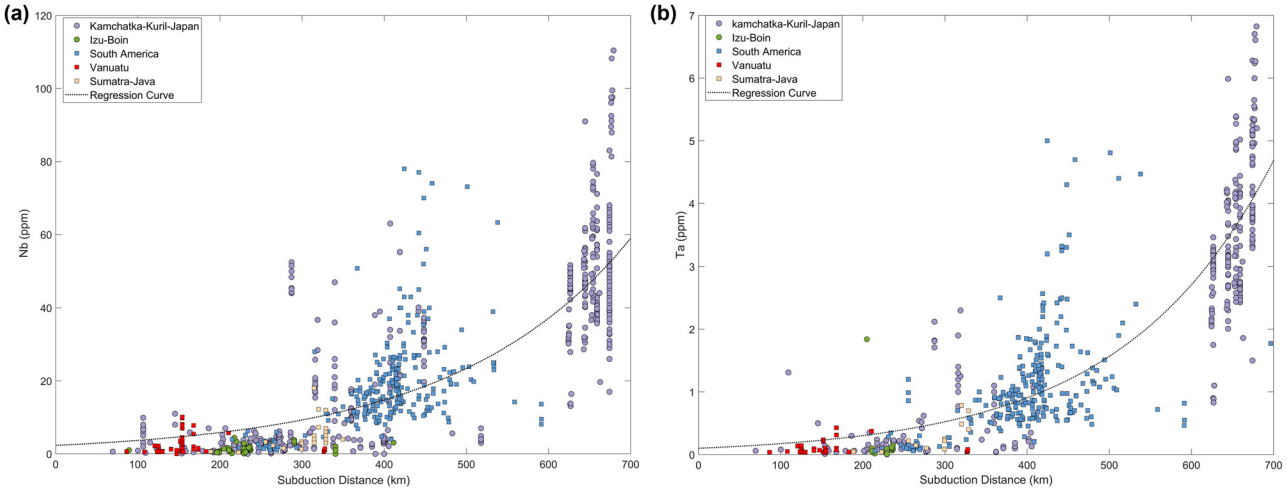

Figure 5: The regression relationship between Nb (a) and Ta (b) concentrations and the subduction distance. The black curve is the regression curve.

which show an increase in trend from ~11 to ~17 with subduction distance in regions of 0–350 km but stayed relatively stable at ~15–18 when subduction distances between 400 and 2,000 with occasional fluctuations (Figure 6). It is worth noting that although the Nb and Ta concentrations of mafic rocks increase rapidly with the distances to subduction zones increase from 350 to 700 km (Figure 5a and b), their Nb/Ta ratios remain relatively constant.

4 Discussion

Several factors may play parts in the Nb and Ta concentrations in mafic rocks, among which Nb–Ta contents of source materials, the degree of partial melting, and possible crustal contamination are key processes that may be responsible for the observed Nb–Ta variation trend with subduction distances. Previous studies [27,67–69] have demonstrated that the dehydration fluid of subducted slab can dissolve little HFSEs such as Nb and Ta at low pressure, while at higher pressure, where key accessory minerals such as rutile start to dissolute in hydrous melt or even supercritical fluids, more Nb and Ta can be dissolved in the fluid and transported to the mantle [30,31,33,34,38,43,70,71]. Therefore, deeper metasomatic fluids would entrain greater Nb and Ta to their overlying mantle wedge and induce partial melting, resulting in higher Nb and Ta concentrations in the source. In a typical modern subduction system, the subduction is in direct proportion to the subduction depth, which provides a first-order explanation for the observed co-variation trends between the Nb–Ta concentrations in mafic rocks and the subduction distances. It is also worth noting that the Nb and Ta concentrations follow the first flat and then gradually changed to steep increasing trends with subduction distances. Such a pattern agrees well with the behavior of HFSE partitioning in the subduction zone fluid, which shows limited mobility at low pressure and increase exponentially with depth at high pressure where accessory minerals such as rutile and Fe–Ti oxides start to dissolve into fluids [72], thus releasing Nb and Ta to the mantle. The established transform pressure for rutile to Ti-clinohumite is ~8 GPa for UHP eclogite, corresponding to the depth of ~250 km, suggesting a possible transform of HFSE mobility in the subduction zone fluids. Experiment studies also indicate that the HFSE contents of low-degree melts increase dramatically with pressures, and the enrichment of Nb and Ta in some OIBs suggesting a partial melting that takes place at depths of >300 km [73]. Therefore, the observed covariation trends of Nb and Ta concentrations in mafic volcanic rocks with their subduction distances may be large because of the pressure difference of their sources. Crustal contamination may also be capable of increasing the Nb and Ta concentrations in the mafic magma, as crustal rocks have significantly higher Nb and Ta concentrations than the mantle rocks [10,11,65,74–84]. However, because the Nb/Ta ratios of crustal rocks are generally

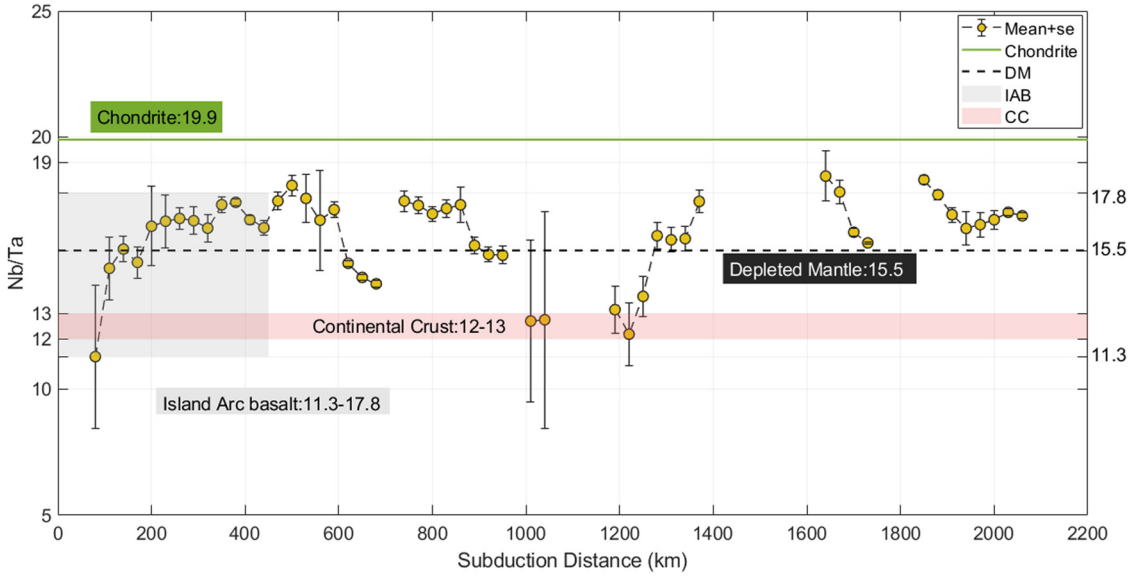

Figure 6: The Nb/Ta ratios' trends of mafic rocks. The yellow circles are mean values corresponding to distance ranging from 0 to 2,200 km (the window width is 60 km and the moving step width is 30 km). Error bars denote one standard error of the mean (SEM).

low [12,27], significant crustal contamination would result in a co-variation trend in Nb vs Nb/Ta, with higher Nb concentrations corresponding to lower Nb/Ta ratios. When the subduction distance is between 350 km and 700 km, the Nb and Ta concentrations continue to increase, but the Nb/Ta ratios are relatively similar, thus indicating insignificant crustal contamination in most of the samples investigated here. The degree of partial melting and fractional crystallization of the studied mafic rocks is unlikely to systematically change with subduction distances, as mafic magmas generally experience less degree of fractional crystallizations.

In respect to Nb/Ta ratios, compared with a DM (~15–17), both CC and arc magmas exhibit low Nb/Ta ratios ~12. However, the exact mechanism for the arc magma and CC to develop low Nb/Ta ratios is vague. Fractionation of Nb and Ta during slab dehydration and transport of hydrous fluid has been proposed to explain the low Nb/Ta ratios in arc magmas [27]. However, others suggest that arclogites with high Nb/Ta ratios (~19) may serve as a counterpart for the formation of arc magmas and CC [85,86]. Nevertheless, a fractionation between Nb and Ta during arc magma formation is observed. In the present study, the Nb/Ta ratios in mafic rocks from arc settings show an increasing trend with the subduction distances (0–350 km), from ~11 to ~17, with relatively low Nb and Ta concentrations. In contrast, in regions dominated by intracontinental magmatism (350–700 km and beyond), Nb and Ta concentrations rapidly increase to high levels with relatively constant mantle-like Nb/Ta ratios. Such a result suggests that, at low pressure, although the releasing fluid has low concentrations of HFSEs such as Nb and Ta, their Nb/Ta ratios seem lower (maybe less than 11) at first with strong crustal signatures. Such a fluid infiltrated and metasomatized the mantle wedge, thus resulting in low Nb/Ta ratios (~11) and low Nb and Ta concentrations in mafic arc rocks that are close to the subduction zones. The increase in Nb/Ta ratios with subduction distances suggests that with the increase in subduction depth, the increase in temperature and pressure would result in smaller Nb–Ta fractionations, and fewer continental crustal signatures. The relatively constant high Nb/Ta ratios in mafic rocks that are far away from subduction zones (distance >350–700 km) suggest limited Nb–Ta fractionation during the slab–fluid interactions at the region. Their Nb/Ta ratios are close to the mantle values supporting the above-discussed idea.

Compared with the traditional geochemical analysis, the numerical performance of Nb–Ta concentrations and regression models in this paper was based on large data and statistical methods. During the data process, we found that data distribution has multi-peak characteristics and does not conform to the normal distribution. We introduced the kernel function estimation method from statistics into the study of geochemical data and propose PDF for data sets without removing the anomalous data, so as to accurately grasp the distribution pattern of the data. The Nb–Ta thresholds were estimated using the CDF, which does not require grouping of the data. Besides, this function will not lose any information, and it is unique for given data sets. In future works, more geochemical indicators can be statistically analyzed. Such attempts and practices may bring new insights into the studies of geochemical cycles and geophysical structures in subduction zones.

5 Conclusion

In this paper, we analyzed the spatial distribution of Nb–Ta in mafic rocks from a statistical perspective by using geophysical models and geochemical data. The upper limit values of Nb–Ta in arc tectonic environments were calculated by CDF. Based on the PDF of Nb–Ta with subduction distance, a regression function model was developed. The following conclusions were obtained.

(1) There are obvious differences in spatial distribution of Nb–Ta concentrations in mafic rocks. That is, arc mafic rocks contain relatively low Nb–Ta concentrations, while the intracontinental mafic rocks contain high Nb–Ta concentrations.
(2) The new geochemical index values of Nb (12.20 ppm) and Ta (0.796 ppm) were proposed to reflect the upper limit of Nb–Ta concentrations in arc tectonic systems based on the CDF. The threshold value can be used as a basic standard for judging whether these mafic rocks are produced by arc tectonic systems.
(3) Nb–Ta concentrations showed a correlation with increasing subduction distance, and the coefficients of R^2 were determined to be 0.679 and 0.773, respectively. As the subduction distance increased, the concentrations of Nb and Ta increased. By contrast, the Nb/Ta ratios do not change significantly, and they remain stable in the range of 12–19.
(4) In our research, the observed covariation trends of Nb and Ta concentrations in mafic rocks with their subduction distances may be large because of the pressure difference of their sources and crustal contamination. However, the relatively similar Nb/Ta ratios along with subduction distances between 350

and 700 km thus suggest insignificant crustal contamination for most of the samples here.

Acknowledgments: This study was supported by Natural Science Foundation of China (Grant No. 41873034, 41703006), National Key R&D Program of China (Grant No. 2016YFC0600404, 2016YFC0600206), and the Fundamental Research Funds for the Central Universities (Grant No. PA2018GDQT0020, JZ2019HGTB0071).

References

[1] Ellam RM, Hawkesworth CJ. Is average continental crust generated at subduction zones? Geology. 1988;16(4):314–7. doi: 10.1130/0091-7613(1988)016<0314:IACCGA>2.3.CO;2.

[2] McCulloch MT, Gamble JA. Geochemical and geodynamical constraints on subduction zone magmatism. Earth Planet Sci Lett. 1991;102(3–4):358–74. doi: 10.1016/0012-821X(91)90029-H.

[3] Bourdon B, Turner S, Dosseto A. Dehydration and partial melting in subduction zones: constraints from U-series disequilibria. J Geophys Res Solid Earth. 2003;108:B6. doi: 10.1029/2002JB001839.

[4] Li HM, Zhai SK, Tao CH, Yu ZH, Ji M. Advances on the magmatism processes in the subduction zones [in Chinese with English abstract]. Adv Mar Sci. 2009;27(1):98–105.

[5] Zheng YF. Metamorphic chemical geodynamics in continental subduction zones. Chem Geol. 2012;328:5–48. doi: 10.1016/j.chemgeo.2012.02.005.

[6] Li HY, Chen RX, Zheng YF, Hu ZC. The crust-mantle interaction in continental subduction channels: zircon evidence from orogenic peridotite in the Sulu orogen. J Geophys Res Solid Earth. 2016;121(2):687–712. doi: 10.1002/2015JB012231.

[7] Cai P, Xu R, Zheng Y, Liu J, Chen X, Yu J. From oceanic subduction to continental collision in North Qaidam: evidence from Kaipinggou orogenic M-type peridotite [in Chinese with English abstract]. Earth Sci. 2018;43(8):2875–92. doi: 10.3799/dqkx.2018.112.

[8] Ma C, Tang YJ, Ying JF. Magmatism in subduction zones and growth of continental crust [in Chinese with English abstract]. Earth Sci. 2019;44(4):1128–42. doi: 10.3799/dqkx.2019.026.

[9] Turcotte DL, Kellogg LH. Isotopic modeling of the evolution of the mantle and crust. Rev Geophys. 1986;24(2):311–28. doi: 10.1029/RG024i002p00311.

[10] Rudnick RL, Fountain DM. Nature and composition of the continental crust: a lower crustal perspective. Rev Geophys. 1995;33(3):267–309. doi: 10.1029/95RG01302.

[11] Plank T, Langmuir CH. The chemical composition of subducting sediment and its consequences for the crust and mantle. Chem Geol. 1998;145(3–4):325–94. doi: 10.1016/S0009-2541(97)00150-2.

[12] Barth MG, McDonough WF, Rudnick RL. Tracking the budget of Nb and Ta in the continental crust. Chem Geol. 2000;165(3–4):197–213. doi: 10.1016/S0009-2541(99)00173-4.

[13] Niu YL, Zhao ZD, Zhu DC, Mo XX. Continental collision zones are primary sites for net continental crust growth – a testable hypothesis. Earth-Sci Rev. 2013;127:96–110. doi: 10.1016/j.earscirev.2013.09.004.

[14] Song SG, Wang MJ, Wang C, Niu YL. Magmatism during continental collision, subduction, exhumation and mountain collapse in collisional orogenic belts and continental net growth: a perspective. Sci China Earth Sci. 2015;58(8):1284–304. doi: 10.1007/s11430-015-5102-x.

[15] Dai LQ, Zhao ZF. Mafic igneous rocks in continental collision orogen record recycling of subducted paleo-oceanic crust [in Chinese with English abstract]. Earth Sci. 2019;44(12):4128–34. doi: 10.3799/dqkx.2019.240.

[16] Liu H, Sun WD, Zartman R, Tang M. Continuous plate subduction marked by the rise of alkali magmatism 2.1 billion years ago. Nat Commun. 2019;10(1):1–8. doi: 10.1038/s41467-019-11329-z.

[17] Zheng YF. Subduction zone geochemistry. Geosci Front. 2019;10(4):1223–54. doi: 10.1016/j.gsf.2019.02.003.

[18] Zhao ZF, Chen RX, Chen YX, Dai LQ, Zheng YF. Progresses in the study of partial melting of ultrahigh-pressure metamorphic rocks and crust-mantle interaction in continental subduction zones [in Chinese with English abstract]. Bull Mineral Petrol Geochem. 2021;40(01):36–59+3-4. doi: 10.19658/j.issn.1007-2802.2021.40.009.

[19] Yu MM, Dilek Y, Yumul GP Jr, Yan Y, Dimalanta CB. Slab-controlled elemental–isotopic enrichments during subduction initiation magmatism and variations in forearc chemostratigraphy. Earth Planet Sci Lett. 2020;538:116217. doi: 10.1016/j.eps1.2020.116217.

[20] Zhai M, Peng P. Origin of early continents and beginning of plate tectonics. Sci Bull. 2020;65(12):970–3. doi: 10.1016lj.scib.2020.03.022.

[21] Cheng QM. Multifractal theory and geochemical element distribution pattern[in Chinese with English abstract]. Earth Sci. 2000;25(3):311–8.

[22] Wei CJ, Zhang YH. Phase transition in the subducted oceanic lithosphere and generation of the subduction zone magma. Chin Sci Bull. 2008;53(23):3603. doi: 10.1007/s11434-008-0405-3.

[23] Chen L, Zhao ZF, Zheng YF. Origin of andesitic rocks: geochemical constraints from Mesozoic volcanics in the Luzong basin, South China. Lithos. 2014;190:220–39. doi: 10.1016/j.lithos.2013.12.011.

[24] Zheng YF, Chen YX, Dai LQ, Zhao ZF. Developing plate tectonics theory from oceanic subduction zones to collisional orogens. Sci China Earth Sci. 2015;58(7):1045–69. doi: 10.1007/s11430-015-5097-3.

[25] Green TH. Significance of Nb/Ta as an indicator of geochemical processes in the crust-mantle system. Chem Geol. 1995;120(3–4):347–59. doi: 10.1016/0009-2541(94)00145-X.

[26] Dostal J, Chatterjee AK. Contrasting behaviour of Nb/Ta and Zr/Hf ratios in a peraluminous granitic pluton (Nova Scotia, Canada). Chem Geol. 2000;163(1–4):207–18. doi: 10.1016/S0009-2541(99)00113-8.

[27] Rudnick RL, Barth M, Horn I,WF. Rutile-bearing refractory eclogites: missing link between continents and depleted

mantle. Science. 2000;287(5451):278–81. doi: 10.1126/science.287.5451.278.
[28] Rapp RP, Shimizu N, Norman MD. Growth of early continental crust by partial melting of eclogite. Nature. 2003;425(6958):605–9. doi: 10.1038/nature02031.
[29] Weyer S, Münker C, Mezger K. Nb/Ta, Zr/Hf and REE in the depleted mantle: implications for the differentiation history of the crust–mantle system. Earth Planet Sci Lett. 2003;205(3–4):309–24. doi: 10.1016/S0012-821X(02)01059-2.
[30] Xiao YL, Sun WD, Hoefs J, Simon K, Zhang ZM, Li SG, et al. Making continental crust through slab melting: constraints from niobium–tantalum fractionation in UHP metamorphic rutile. Geochim Cosmochim Acta. 2006;70(18):4770–82. doi: 10.1016/j.gca.2006.07.010.
[31] Zhang ZM, Shen K, Sun WD, Liu YS, Liou JG, Shi G, et al. Fluids in deeply subducted continental crust: petrology, mineral chemistry and fluid inclusion of UHP metamorphic veins from the Sulu orogen, eastern China. Geochim Cosmochim Acta. 2008;72(13):3200–28. doi: 10.1016/j.gca.2008.04.014.
[32] Ding X, Lundstrom C, Huang F, Li J, Zhang ZM, Sun XM, et al. Natural and experimental constraints on formation of the continental crust based on niobium–tantalum fractionation. Int Geol Rev. 2009;51(6):473–501. doi: 10.1080/00206810902759749.
[33] Beinlich A, Klemd R, John T, Gao J. Trace-element mobilization during Ca-metasomatism along a major fluid conduit: eclogitization of blueschist as a consequence of fluid–rock interaction. Geochim Cosmochim Acta. 2010;74(6):1892–922. doi: 10.1016/j.gca.2009.12.011.
[34] Huang J, Xiao YL, Gao Y, Hou ZH, Wu W. Nb–Ta fractionation induced by fluid-rock interaction in subduction-zones: constraints from UHP eclogite-and vein-hosted rutile from the Dabie orogen, Central-Eastern China. J Metamorphic Geol. 2012;30(8):821–42. doi: 10.1111/j.1525-1314.2012.01000.x.
[35] Liu L, Xiao YL, Aulbach S, Li DY, Hou ZH. Vanadium and niobium behavior in rutile as a function of oxygen fugacity: evidence from natural samples. Contrib Mineral Petrol. 2014;167(6):1026. doi: 10.1007/s00410-014-1026-2.
[36] Chen YX, Zheng YF. Extreme Nb/Ta fractionation in metamorphic titanite from ultrahigh-pressure metagranite. Geochim Cosmochim Acta. 2015;150:53–73. doi: 10.1016/j.gca.2014.12.002.
[37] Peng SB, Liu SF, Lin MS, Wu CF, Hang QS. Early Paleozoic subduction in Cathaysia (II): new evidence from the Dashuang high magnesian-magnesian andesite[in Chinese with English abstract]. Earth Sci. 2016;41(6):931–47. doi: 10.3799/dqkx.2016.079.
[38] Tan DB, Li DY, Xiao YL. Geochemical characteristics of niobium and tantalum: a review of twin elements [in Chinese with English abstract]. Earth Sci. 2018;43(1):317–32. doi: 10.3799/dqkx.2018.019.
[39] Zheng YF, Xu Z, Chen L, Dai LQ, Zhao ZF. Chemical geodynamics of mafic magmatism above subduction zones. J Asian Earth Sci. 2020;194:104185. doi: 10.1016/j.jseaes.2019.104185.
[40] Stalder R, Foley SF, Brey GP, Horn I. Mineral-aqueous fluid partitioning of trace elements at 900–1,200°C and 3.0–5.7 GPa: new experimental data for garnet, clinopyroxene, and rutile, and implications for mantle metasomatism. Geochim Cosmochim Acta. 1998;62(10):1781–801. doi: 10.1016/s0016-7037(98)00101-x.
[41] Klemme S, Blundy JD, Wood BJ. Experimental constraints on major and trace element partitioning during partial melting of eclogite. Geochim Cosmochim Acta. 2002;66(17):3109–23. doi: 10.1016/S0016-7037(02)00859-1.
[42] Zack T, Kronz A, Foley SF, Rivers T. Trace element abundances in rutiles from eclogites and associated garnet mica schists. Chem Geol. 2002;184(1–2):97–122. doi: 10.1016/S0009-2541(01)00357-6.
[43] John T, Gussone N, Podladchikov YY, Bebout GE, Dohmen R, Halama R, et al. Volcanic arcs fed by rapid pulsed fluid flow through subducting slabs. Nat Geosci. 2012;5(7):489–92. doi: 10.1038/ngeo1482.
[44] Wu CL, Liu G. Big data and future development of geological science [in Chinese with English abstract]. Geol Bull China. 2019;38(7):1081–8.
[45] Gray J, Szalay A. eScience-A transformed scientific method. Mountain View, CA: Presentation to the Computer Science and Technology Board of the National Research Council; 2007.
[46] Hey T, Tansley S, Tolle K. The fourth paradigm: data-intensive-scientific discovery. Redmond: Microsoft Research; 2009.
[47] Mayer-Schonberger V, CuKier K. Big data: a revolution that will transform how we live, work and think. New York: Houghton Mifflin Harcourt Publishing Company; 2013.
[48] EarthChem. Portal search: www.earthchem.org/portal; 2017.
[49] Nohl U, Sarbas B. GEOROC, the MPI geochemical rock database: introduction of the Web interface. AGU fall meeting; 1999.
[50] Van der Hilst RD, Widiyantoro S, Engdahl ER. Evidence for deep mantle circulation from global tomography. Nature. 1997;386(6625):578–84. doi: 10.1038/386578a0.
[51] Kellogg LH, Hager BH, van der Hilst RD. Compositional stratification in the deep mantle. Science. 1999;283(5409):1881–4. doi: 10.1126/science.283.5409.1881.
[52] Zhang CL, Zou HB. Permian A-type granites in Tarim and western part of Central Asian orogenic belt (CAOB): genetically related to a common Permian mantle plume? Lithos. 2013;172:47–60. doi: 10.1016/j.lithos.2013.04.001.
[53] Madsen JK, Thorkelson DJ, Friedman RM, Marshall DD. Cenozoic to recent plate configurations in the Pacific Basin: ridge subduction and slab window magmatism in western North America. Geosphere. 2006;2(1):11–34. doi: 10.1130/GES00020.1.
[54] Thorkelson DJ. Subduction of diverging plates and the principles of slab window formation. Tectonophysics. 1996;255(1–2):47–63. doi: 10.1016/0040-1951(95)00106-9.
[55] Defant MJ, Drummond MS. Derivation of some modern arc magmas by melting of young subducted lithosphere. Nature. 1990;347(6294):662–5. doi: 10.1038/347662a0.
[56] Norton IO. Plate motions in the North Pacific: the 43 Ma nonevent. Tectonics. 1995;14(5):1080–94. doi: 10.1029/95TC01256.
[57] Hayes GP, Moore GL, Portner DE, Hearne M, Flamme H, Furthey M, et al. Slab2, a comprehensive subduction zone geometry model. Science. 2018;362(6410):58–61. doi: 10.1126/science.aat4723.
[58] Portner DE, Hayes GP. Incorporating teleseismic tomography data into models of upper mantle slab geometry. Geophys J Int. 2018;215(1):325–32. doi: 10.1093/gji/ggy279.

[59] Ge C, Wang FY, Li YD, Li XH, Li XY, Zhou YZ, et al. Analysis of geochemical indices of crustal thickness based on GEOROC big data [in Chinese with English abstract]. Acta Petrol Sin. 2018;34(11):3179–88.
[60] Lu Z, Shao XB. Research on the diving plate shape characteristic of global diving belt [in Chinese with English abstract]. Seismol Res Northeast China. 2004;3(20):17–25. doi: 10.3969/j.issn.1674-8565.2004.03.003.
[61] Li CY, Xing JX, Li DY, Gong W, Guo YF, Li CY. Spatial difference and its impact on the subduction characteristics of the Kuril–Kamchatka subduction zone [in Chinese with English abstract]. Mar Sci. 2018;42(8):1–13. doi: 10.11759/hykx20170809002.
[62] Liu Z, Jianghai LI, Cui X, Yun X, Fan Q. Geometry of Aleutian subduction zone and its kinematic genesis [in Chinese with English abstract]. Geol Rev. 2018;64(3):543–550. doi: 10.16509/j.georeview.2018.03.002.
[63] Hofmann AW. Chemical differentiation of the Earth: the relationship between mantle, continental crust, and oceanic crust. Earth Planet Sci Lett. 1988;90(3):297–314. doi: 10.1016/0012-821X(88)90132-X.
[64] Workman RK, Hart SR. Major and trace element composition of the depleted MORB mantle (DMM). Earth Planet Sci Lett. 2005;231(1–2):53–72. doi: 10.1016/j.epsl.2004.12.005.
[65] Münker C, Pfänder JA, Weyer S, Büchl A, Kleine T, Mezger K. Evolution of planetary cores and the Earth–Moon system from Nb/Ta systematics. Science. 2003;301(5629):84–7. doi: 10.1126/science.1084662.
[66] Münker C, Wörner G, Yogodzinski G, Churikova T. Behaviour of high field strength elements in subduction zones: constraints from Kamchatka–Aleutian arc lavas. Earth Planet Sci Lett. 2004;224(3–4):275–93. doi: 10.1016/j.epsl.2004.05.030.
[67] Hermann J, Rubatto D. Accessory phase control on the trace element signature of sediment melts in subduction zones. Chem Geol. 2009;265(3–4):512–26. doi: 10.1016/j.chemgeo.2009.05.018.
[68] Baier J, Audétat A, Keppler H. The origin of the negative niobium tantalum anomaly in subduction zone magmas. Earth Planet Sci Lett. 2008;267(1–2):290–300. doi: 10.1016/j.epsl.2007.11.032.
[69] Janasi VA. Elemental and Sr–Nd isotope geochemistry of two Neoproterozoic mangerite suites in SE Brazil: implications for the origin of the mangerite–charnockite–granite series. Precambrian Res. 2002;119(1–4):301–27. doi: 10.1016/S0301-9268(02)00127-4.
[70] Gao J, John T, Klemd R, Xiong XM. Mobilization of Ti–Nb–Ta during subduction: evidence from rutile-bearing dehydration segregations and veins hosted in eclogite, Tianshan, NW China. Geochim Cosmochim Acta. 2007;71(20):4974–96. doi: 10.1016/j.gca.2007.07.027.
[71] John T, Klemd R, Gao J, Garbe-Schönberg CD. Trace-element mobilization in slabs due to non steady-state fluid-rock interaction: constraints from an eclogite-facies transport vein in blueschist (Tianshan, China). Lithos. 2008;103(1–2):1–24. doi: 10.1016/j.lithos.2007.09.005.
[72] Xiong X, Keppler H, Audétat A, Gudfinnsson G, Sun WD, Song MS, et al. Experimental constraints on rutile saturation during partial melting of metabasalt at the amphibolite to eclogite transition, with applications to TTG genesis. Am Mineral. 2009;94(8–9):1175–86. doi: 10.2138/am.2009.3158.
[73] Spandler C, Hermann J, Faure K, Mavrogenes JA, Arculus RJ. The importance of talc and chlorite "hybrid" rocks for volatile recycling through subduction zones; evidence from the high-pressure subduction mélange of new Caledonia. Contrib Mineral Petrol. 2008;155(2):181–98. doi: 10.1007/s00410-007-0236-2.
[74] Shaw DM, Reilly GA, Muysson JR, Pattenden GE, Campbell FE. An estimate of the chemical composition of the Canadian Precambrian shield. Can J Earth Sci. 1967;4(5):829–53. doi: 10.1139/e67-058.
[75] Shaw DM, Dostal J, Keays RR. Additional estimates of continental surface Precambrian shield composition in Canada. Geochim Cosmochim Acta. 1976;40(1):73–83. doi: 10.1016/0016-7037(76)90195-2.
[76] Weaver BL, Tarney J. Empirical approach to estimating the composition of the continental crust. Nature. 1984;310(5978):575–7. doi: 10.1038/310575a0.
[77] Rudnick RL, Taylor SR. The composition and petrogenesis of the lower crust: a xenolith study. J Geophys Res Solid Earth. 1987;92(B13):13981–4005. doi: 10.1029/JB092iB13p13981.
[78] Condie KC. Chemical composition and evolution of the upper continental crust: contrasting results from surface samples and shales. Chem Geol. 1993;104(1–4):1–37. doi: 10.1016/0009-2541(93)90140-E.
[79] Shaw DM, Dickin AP, Li H, Mcnutt R, Schwarcz H, Truscott MG. Crustal geochemistry in the Wawa-Foleyet region, Ontario. Can J Earth Sci. 1994;31(7):1104–21. doi: 10.1139/e94-099.
[80] Gao S, Luo TC, Zhang BR, Zhang HF, Han YW, Zhao ZD, et al. Chemical composition of the continental crust as revealed by studies in East China. Geochim Cosmochim Acta. 1998;62(11):1959–75. doi: 10.1016/S0016-7037(98)00121-5.
[81] Taylor SR, McLennan SM. The continental crust: its composition and evolution. Oxford: Blackwell Scientific; 1985.
[82] Taylor SR, McLennan SM. The geochemical evolution of the continental crust. Rev Geophys. 1995;33(2):241–65. doi: 10.1029/95RG00262.
[83] Wedepohl KH. The composition of the continental crust. Geochim Cosmochim Acta. 1995;59(7):1217–32. doi: 10.1016/0016-7037(95)00038-2.
[84] Rudnick R, Gao S. Composition of the continental crust. Crust. 2014;3:1–64. doi: 10.1016/B978-0-08-095975-7.00301-6.
[85] Jagoutz O, Behn M. Foundering of lower island-arc crust as an explanation for the origin of the continental Moho. Nature. 2013;504:131–4. doi: 10.1038/nature12758.
[86] Tang M, Lee CTA, Chen K, Erdman M, Costin G, Jiang HH. Nb/Ta systematics in arc magma differentiation and the role of arclogites in continent formation. Nat Commun. 2019;10(1):1–8. doi: 10.1038/s41467-018-08198-3.